CrystEngComm

Accepted Manuscript

ROYAL SOCIETY OF CHEMISTRY

www.rsc.org/crystengcomm

CrystEngComm RSCPublishing

ARTICLE

Enhanced Thermoelectric Performance of GeTe-rich Germanium Antimony Tellurides Through the Control of Composition and Structure

Cite this: DOI: 10.1039/x0xx00000x

Received 00th January 2012,
Accepted 00th January 2012

DOI: 10.1039/x0xx00000x

www.rsc.org/

Raman Sankar,[a] Chiao-Song Chi,[b] Deniz P. Wong,[b] Wei-Lun Chien,[c] Jih-Shang Hwang,[c] Fang-Cheng Chou,[a] Li-Chyong Chen[a*] and Kuei-Hsien Chen[b*]

Germanium antimony telluride (GeSbTe or GST), a popular material in optical and non-volatile memory devices, attracted renewed attention due to its potential for thermoelectric applications. In this study, we have employed two-stage engineering process to enhance the thermoelectric properties of GeTe-rich GeSbTe. First, we introduced vacancy to the material by modifying the germanium content without disrupting the crystal structure. This influenced the electronic properties of the GeTe-rich GeSbTe and improved the overall dimensionless figure of merit, zT, from 0.7 to 1.1. Second, we rapidly cooled the material after annealing, further enhancing the zT value from 1.1 to 1.48–one of the highest values reported for this material. In-depth studies suggest that disorder in the crystal structure created via rapid cooling enhanced phonon scattering and effectively reduced the thermal conductivity, which, in turn, enhanced thermoelectric performance.

Introduction

Since the discovery of thermoelectric effect centuries ago,[1,2] people have invested a lot of effort in harnessing useful energy from waste heat. It is clean, sustainable and environmental friendly. However, thermoelectric devices have been saddled by low efficiency.[3] Better materials, useful architectures and new strategies to improve thermoelectric efficiency are important for the commercialization of the technology. The thermoelectric efficiency can be measured by the dimensionless figure of merit, zT; the higher the zT, the better the thermoelectric efficiency. By definition, $zT = (S^2\sigma T)/\kappa$, and an optimum efficiency can be obtained from proper balance among three physical parameters: Seebeck coefficient (S), electrical conductivity (σ) and thermal conductivity (κ) at certain operating temperature (T). Currently, chalcogenide-based compounds (materials containing the sulfur, selenium and tellurium) offer the highest thermoelectric performance based from the reported dimensionless figure of merit, zT.[4-6] Among those, lead tellurides[7,8] and tin selenides[9] reach zT of more than 2. Unfortunately, lead tellurides suffer from the problem of toxicity while tin selenides are structurally complex. Furthermore, integrating new materials in actual devices requires intensive studies of the suitable electrical contacts,[10,11] reasonable mechanical stability,[12] and appropriate device architecture.[13,14] Thus, search for a better material is still a premium in thermoelectric research.

Germanium-antimony-tellurium (GeSbTe or GST) stands out as a potential material in thermoelectric applications. This class of material is originally utilized in optical and non-volatile memory devices because of its phase change properties.[15,16] Coincidentally, the properties that are advantageous in the aforementioned application, like small band gap and low thermal conductivity, are also suitable for thermoelectric applications.[17,18] Moreover, given that this material has long been integrated in memory device fabrication, infrastructures are already in place if ever GeSbTe develops into a viable active material in thermoelectric devices. Thus, further improving the thermoelectric properties of the GeSbTe offers an attractive avenue for commercialization in the future.

Current research of GeSbTe as a thermoelectric material focuses on exploring the material system by looking at crystal structure,[19] composition,[20] effects of adding another element[21] and post-crystal growth treatment.[22] Recent activities reported for this material have encourage us that there are still a lot of room for improvement in this material system.

GeSbTe exists in various compositions and crystal structures giving different physical properties that affect their functions.[23-25] Rosenthal et al. previously demonstrated that rapidly cooled GeTe-rich GeSbTe—composed of mixed crystal structures—show the best thermoelectric performance.[19] GeTe-rich GeSbTe refers to material composition dominantly GeTe as elucidated from the pseudo-binary phase diagram of GeTe and Sb_2Te_3.[26] In this work, we further enhance the Seebeck coefficient and reduce thermal conductivity by a two-step process: (1) introducing vacancy by marginally perturbing the composition of the GeTe-rich GeSbTe and (2) incorporating mixed crystal structures by rapid cooling technique.

EXPERIMENTAL

GeSbTe crystal growth

Polycrystalline GeSbTe compounds were prepared by solid state reaction. High-purity starting elements of Ge (99.999%, powder), Sb (99.9999%, shot), Te (99.999%, chunks) and Te (99.999%, shot), were melted in carbon-coated quartz tubes with diameter of 1.6 cm under vacuum at 950 °C for 24 hrs., then slowly cooled to 500 °C, followed by a rapid quenching in water. The obtained ingots were pulverized to powder, then sealed in quartz tubes under a vacuum of about 10^{-4} Torr after multiple argon gas purging cycles, and pretreated at 650 °C for 18 hrs. in a box furnace. After cooling to room temperature, single crystals were grown from the pre-treated powder with a vertical Bridgman furnace and vacuum sealed in carbon coated quartz tubes of 10 cm in length and 1.6 cm in diameter. The temperature profile of the Bridgman furnace used for the whole series was maintained at 500–950 °C within a 25 cm. region. Initial complete melting was achieved at 950 °C for 24 hrs. to ensure complete reaction and mixing. A temperature gradient of 1 °C/cm was programmed around the solidification point near 700 °C, and the quartz tube was then slowly lowered into the cooling zone at a rate of ~0.5 mm/h. The pristine sample is labelled GST. Introduction of vacancy was achieved by tuning the initial composition ratio of Ge, Sb and Te; this sample is labelled as V-GST. For the rapidly cooled samples, the quartz tube containing the material was removed from the furnace when the temperature reached 500 °C. The pristine sample was labelled as GST-air quenched and the modified sample was labelled V-GST-air quenched. The obtained crystalline ingots were cut and polished into rectangular shapes of approximately 3x3x12 mm^3 for Seebeck coefficient and electrical conductivity measurements while a circular disc of a diameter of 12 mm and a thickness of 2 mm was used for thermal diffusivity measurements.

Material Characterization

Fractured surface morphology was observed using field emission scanning electron microscopy (FESEM, JEOL6700). The chemical composition of the as-prepared ingots was determined using energy dispersive X-ray spectrometry (Oxford) attached to the SEM. The crystal lattice was observed using field emission transmission electron microscopy (FEG-TEM, JEOL2100). X-ray diffraction (XRD) pattern was obtained from Bruker D8 with CuKα irradiation. The Hall measurement was obtained at room temperature under 0.55 T with a four-probe configuration using the van der Pauw method (ECOPIA HMS-5000). The electrical conductivity and the Seebeck coefficient were measured simultaneously using commercial equipment (ZEM-3, ULVAC-RIKO, Japan) in a He atmosphere from 300 to 700 K. The thermal conductivity was calculated from the equation $\kappa = D \times Cp \times d$, where the thermal diffusivity, D, was obtained using a laser flash apparatus (NETZSCH, LFA 457), specific heat, Cp, was determined using a differential scanning calorimeter (SETARAM, TG-DSC111), and the density, d, was obtained using the Archimedes method. The density of the samples is measured to be 5.90 g/cm3 with less than 1% variation from sample to sample.

RESULT AND DISCUSSION

GeTe-rich GeSbTe crystals

The solid state reaction produces highly dense metallic dark silver ingots (Fig. 1(a)), which demonstrates good stability in water and air. Morphological features of the free-fracture surface of the ingot (Fig. 1(b)) reveal a highly faceted layer-like structure consistent with literature report.[27] Furthermore, the observed triangular shape morphology indicates a three-fold symmetry crystal structure which is verified from the XRD pattern (Fig. 2(a)). The dominant phase observed from XRD suggests a rhombohedral crystal structure belonging to the trigonal crystal system similar to GeTe, as indicated by the reference powder diffraction file. This also indicates that we obtained GeTe-rich GeSbTe, which is in accordance with the pseudo-binary phase diagram of GeTe and Sb_2Te_3 compounds.[26, 28-29] Fig. 2(b) shows a characteristic endothermic peak at 600 K, pertaining to the transition temperature of GeTe-rich GeSbTe. The identified transition temperature enables us to qualitatively locate the position of our sample in the phase diagram, which indeed points to a GeTe-rich GeSbTe. These results corroborate those of Rosenthal *et al*.[19]

Thermoelectric properties of GeSbTe crystals

In order to assess the thermoelectric performance of our GeTe-rich GeSbTe samples, we obtained the Seebeck coefficient (S), electrical conductivity (σ) and thermal conductivity (κ) (Fig. 3). Between the pristine GST and V-GST, the figure shows that the latter has higher Seebeck coefficient—with a compromised electrical conductivity. Nonetheless, this still gives an overall higher power factor (P.F.), where P.F. = $S^2\sigma$. Similar observations can be inferred from the air quenched samples. Looking at the thermal transport property (Fig. 3(d)), V-GST possesses lower thermal conductivity compared to GST. In addition, all air quenched samples exhibits lower thermal conductivity compared with their pristine counterparts.

The highest zT value achieved (Fig. (4)) is 1.48, one of the highest numbers for this class of material. The V-GST-air quenched exhibited the highest zT value at 673K followed by GST-air quenched and V-GST. The results show that the sample with perturbed composition offered the best performance and that the efficiency can be further enhanced by simply quenching the sample at room temperature in air atmosphere.

Effect of vacancy

The composition analysis shows that the Ge concentration is slightly perturbed through the removal of some Ge prior to growth. However, they are not enough to disrupt the crystal structure of the sample (GST vs. V-GST) as observed from their XRD pattern in Fig. 5. Despite the similarities, the thermoelectric properties of both samples indicate otherwise.

In order to explain the effects of the material to its thermoelectric parameters, we have measured several key parameters to describe their electronic properties (Table 1). Using our Hall measurement system, we determined the carrier concentration and carrier mobility and derived the effective mass through the relationship of Seebeck coefficient with carrier concentration of the material as indicated by this equation:[30-32]

$$S = \frac{8\pi^2 K_B^2}{3eh^2} m^* T \left(\frac{\pi}{3\eta}\right)^{\frac{2}{3}} \qquad \text{(Eq. 1)}$$

where K_B refers to the Boltzmann constant, e the electric charge, h the Planck constant, m* the effective mass and η the carrier concentration. This equation is based on the Mott expression[32] and assumes that the material is metallic-like or degenerate semiconductor. From our carrier concentration values, we can conclude that our GeTe-rich GeSbTe samples have this characteristics.

The better electrical conductivity from the GST sample can be accounted to its higher carrier mobility compared to V-GST, which at the same time created a compromise with the carrier concentration of the materials. This translates to a higher effective mass for the V-GST sample. We initially hypothesized that introducing more vacancy into the system would lead to larger effective mass. By definition, effective mass is the particle's mass as a response to electric field.[33] The sample with more vacancy in effect would have larger effective force field acting upon the carrier particle thus exhibiting a larger effective mass. From the previous equation, this translates to larger Seebeck coefficient. Thus, increase in zT value from 0.7 to 1.1 at 670K was observed for GST and V-GST samples, respectively.

The result indicates that a marginal perturbation in the composition of GeTe-rich GeSbTe can significantly influence the electronic properties of the material without affecting their crystal structure. Thus, we can tune the thermoelectric properties of this material by carefully changing the Ge composition of the compound. At the same time, it should be noted how the composition of GeTe-rich GeSbTe is sensitive to its electronic properties. Therefore, we also need to develop an efficient control of the composition in the future.

Effect of rapid cooling

Rapidly cooling the sample during the end step of the growth process allowed us to obtain a sample with more mixed crystal structures (Fig. 5). As the figure suggests, V-GST air quenched sample contains more prominent peak (at 42.65°) associated with the cubic crystal structure.[34] The increased presence of the cubic structure influences the Seebeck coefficient and electrical conductivity of the material. However, the power factor did not change significantly. On the other hand, the effect of rapid cooling mainly affects the thermal conductivity of the materials. From the TEM images (Fig. 6), the sample that underwent quenching exhibited a more disordered crystal lattice with a more diffused SAED pattern. This indicates the presence of "defect layers" as observed previously.[19] Since our sample underwent rapid cooling in air, we observed a more disordered structure in contrast to the ordered parquet-like structure found in the water-quenched sample.[19] The slower quenching rate could have possibly randomly trapped the high temperature cubic structure instead of the more ordered arrangement of the "defect layers" as observed by the previous group. The increase in randomness provided a lower thermal conductivity, which increased the zT value of our GeTe-rich GeSbTe sample to 1.48 at 670 K.

Conclusions

In conclusion, we demonstrated a two-step enhancement in the thermoelectric performance of GeTe-rich GeSbTe. Firstly, via fine tuning the Ge composition, the dimensionless figure of merit, zT, was enhanced from 0.7 to 1.1. This is believed to be caused by the presence of vacancy in the material system that influences the effective mass which translates to improve power factor. Secondly, via effective rapid cooling of the samples, 40% reduction of the thermal conductivity has been achieved, which leads to 100% enhancement in zT with a maximum value of 1.48 at 670 K. Detailed characterization and analysis conclude that the thermoelectric parameter of GeTe-rich GeSbTe is sensitive to its composition: a marginal change in composition can drastically alter the outcome of the thermoelectric property. Furthermore, by rapidly cooling the sample in air instead of water, we were able to create a more disordered lattice system that accounts for the reduction of thermal conductivity. We believe this study on GeTe-rich GeSbTe samples can provide a blueprint for future design of the material for thermoelectric applications with ultimate zT values.

Acknowledgements

The authors would like to thank Mr. T.W. Lan and Dr. Y.Y. Chen for part of thermoelectric property measurement and technical support by Nano Core Facility Center in Academia Sinica. Financial support by Center for Sustainability Science in Academia Sinica, Taiwan is gratefully acknowledged.

Notes and references

[a] Center for Condensed Matter Sciences, National Taiwan University, Taipei 106, Taiwan, E-mail: chenlc@ntu.edu.tw (LCC)

[b] Institute of Atomic and Molecular Science, Academia Sinica, Taipei 106, Taiwan, E-mail: chenkh@pub.iams.sinica.edu.tw (KHC)
[c] Institute of Optoelectronic Sciences, National Taiwan Ocean University, Keelung 202, Taiwan

† Footnotes should appear here. These might include comments relevant to but not central to the matter under discussion, limited experimental and spectral data, and crystallographic data.

Electronic Supplementary Information (ESI) available: [details of any supplementary information available should be included here]. See DOI: 10.1039/b000000x/

1 E. Altenkirch, *Phys. Z.*, 1909, **10**, 560.
2 E. Altenkirch, *Phys. Z.*, 1911, **12**, 920.
3 L.E. Bell, *Science*, 2008, **321**, 1457.
4 H. Wang, J.H. Bahk, C. Kang, J. Hwang, K. Kim, J. Kim, P. Burke, J.E. Bowers, A.C. Gossard, A. Shakouri and W. Kim, *Proc. Natl. Acad. Sci. USA,* 2014, **111**, 10949.
5 A.P. Gonçalves and C. Godart, Eur. Phys. J. B 2014, **87**, 1-29.
6 L.D. Zhao, V.P. Dravid and M.G. Kanatzidis, *Energy Environ. Sci.*, 2014, **7**, 251.
7 K. Biswas, J. He, I.D. Blum, C.I. Wu, T.P. Hogan, D.N. Seidman, V.P. Dravid and M.G. Kanatzidis, *Nature*, 2012, **489**, 414.
8 L.D. Zhao, H.J. Wu, S.Q. Hao, C.I. Wu, X.Y. Zhou, K. Biswas, J.Q. He, T.P. Hogan, C. Uher, C. Wolverton, V.P. Dravid, and M.G. Kanatzidis, *Energy Environ. Sci.*, 2013, **6**, 3346.
9 L.D. Zhao, S.H. Lo, Y. Zhang, H. Sun, G. Tan, C. Uher, C. Wolverton, V.P. Dravid and M.G. Kanatzidis, *Nature*, 2014, **508**, 373.
10 O. Yamashita, *J. Appl. Phys.*, 2004, **95**, 178.
11 Y. Gao, A.M. Marconnet, M.A. Panzer, S. LeBlanc, S. Dogbe, Y. Ezzahri, A. Shakouri and K.E. Goodson, *J. Electron. Mater.*, 2010, **39**, 1456.
12 Y. Gelbstein, Z. Dashevsky, and M.P. Dariel, *J. Appl. Phys.*, 2008, **104**, 03370201.
13 M. Hodes, *IEEE T. Compon. Pack. T.*, 2007, **30**, 50.
14 K. Yazawa and A. Shakouri, *J. Appl. Phys.*, 2012, **111**, 02450901.
15 Y.J. Huang, M.C. Tsai, C.H. Wang and T.E. Hsieh, *Thin Solid Films*, 2012, **520**, 3692.
16 C. Xu, B. Liu, Z. Song, S. Feng and B. Chen, *Thin Solid Films*, 2008, **516**, 7871.
17 M.N. Schneider, T. Rosenthal, C. Stiewe and O. Oeckler, *Z. Kristallogr.*, 2010, **225**, 463.
18 T. Rosenthal, P. Urban, K. Nimmrich, L. Schenk, J. de Boor, C. Stiewe and O. Oeckler, *Chem. Mater.*, 2014, **26**, 2567.
19 T. Rosenthal, M.N. Schneider, C. Stiewe, M. Döblinger and O. Oeckler, *Chem. Mater.*, 2011, **23**, 4349.
20 K.S. Siegert, F.R. Lange, E.R. Sittner, H. Volker, C. Schlockermann, T. Siegrist and M Wuttig, *Rep. Prog. Phys.*, 2015, **78**, 013001.
21 S. Welzmiller, T. Rosenthal, P. Ganter, L. Neudert, F. Fahrnbauer, P. Urban, C. Stiewe, J. de Boor and O. Oeckler, *Dalton Trans.*, 2014, **43**, 10529.
22 A. Kosuga, K. Nakai, M. Matsuzawa, Y. Fujii, R. Funahashi, T. Tachizawa, Y. Kubota, and K. Kifune, *J. Alloys Compds.*, 2015, **618**, 463.
23 N. Yamada and T. Matsunaga, *J. Appl. Phys.*, 2000, **88**, 7020.
24 B.S. Lee, J.R. Abelson, S.G. Bishop, D.H. Kang, B.K. Cheong and K.B. Kim, *J. Appl. Phys.*, 2005, **97**, 09350901.
25 J. Akola and R.O. Jones, *Phys. Rev. B*, 2007, **76**, 23520101.
26 N. Yamada, E. Ohno, K. Nishiuchi, N. Akahira and M. Takao, *J. Appl. Phys.*, 1991, **69**, 2849.
27 M. N. Schneider, P. Urban, A. Leineweber, M. Döblinger and O. Oeckler, *Phys. Rev. B* 2010, **81**, 18410201.
28 B. Legendre, C. Hancheng, S. Bordas and M.T. Clavaguera-Mora, *Thermochim. Acta,* 1984, **78**, 141.
29 S. Bordas, M.T. Clavaguer-Mora, B. Legendre and C. Hancheng, *Thermochim. Acta*, 1986, **107**, 239.
30 M. Cutler, J.F. Leavy and R. L. Fitzpatrick, *Phys. Rev.* 1964, **133**, A1143.
31 G. J. Snyder and E.S. Toberer, *Nat. Mater.* 2008, **7**, 105.
32 J. P. Heremans, V. Jovovic, E.S. Toberer, A. Saramat, K. Kurosaki, A. Charoenphakdee, S. Yamanaka and G.J. Snyder, *Science*, 2008, **321**, 554.
33 C. Kittel, *Introduction to Solid State Physics.* 8th ed.; John Wiley & Sons, Inc.: United States of America, 2005.
34 T. Matsunaga, N. Yamada and Y. Kubota, *Acta Crystallogr. B*, 2004, **60**, 685.

CrystEngComm RSCPublishing

ARTICLE

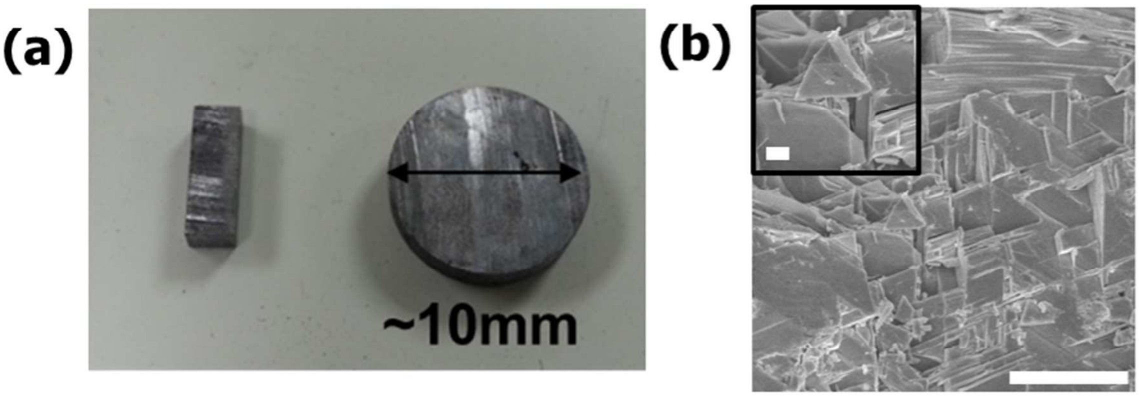

Fig. 1 Photographic image and scanning electron micrograph of the GeTe-rich GeSbTe samples used for this study. Scale bar for the SEM image is 10 µm and 1 µm for the inset.

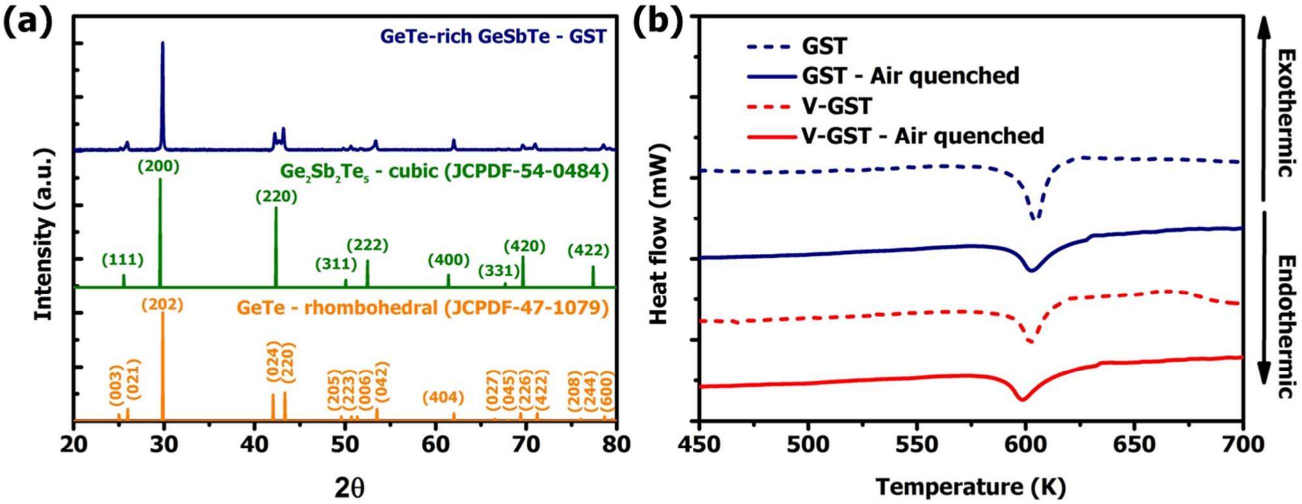

Fig. 2 (a) X-ray diffraction pattern and (b) Differential scanning calorimetric profile of the GeTe-rich GeSbTe samples.

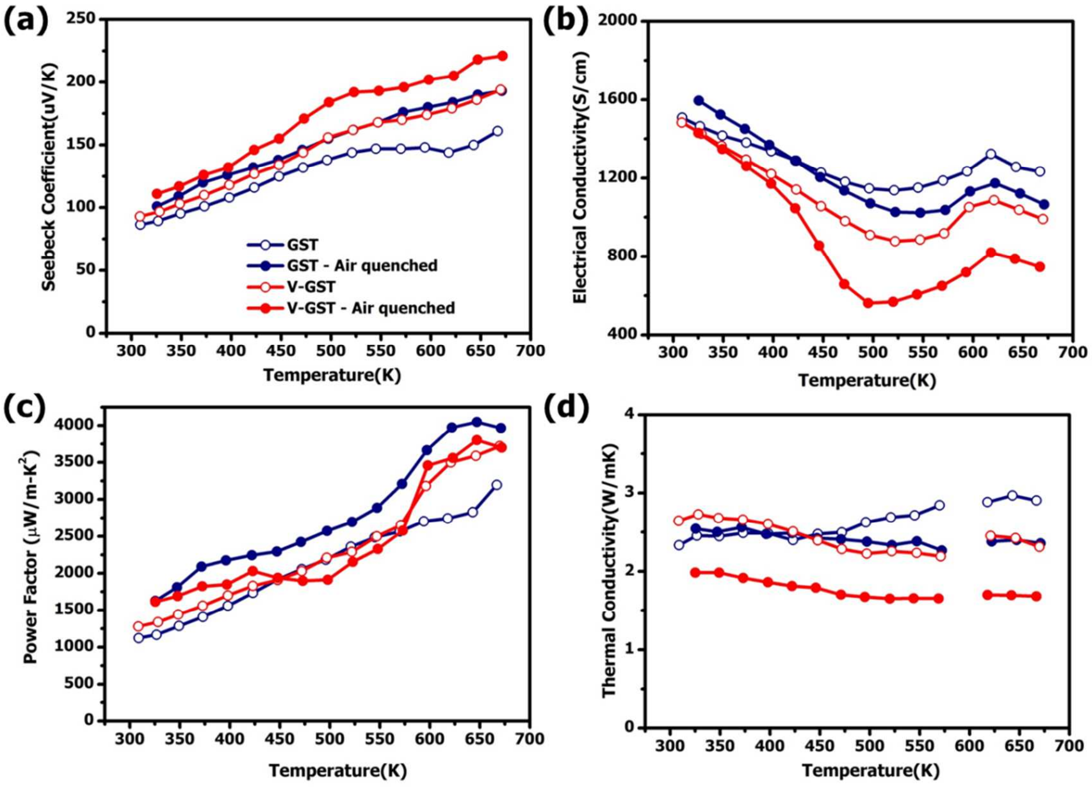

Fig. 3 Temperature dependence of (a) Seebeck coefficient, (b) electrical conductivity, (c) power factor and (d) thermal conductivity of GeTe-rich GeSbTe samples.

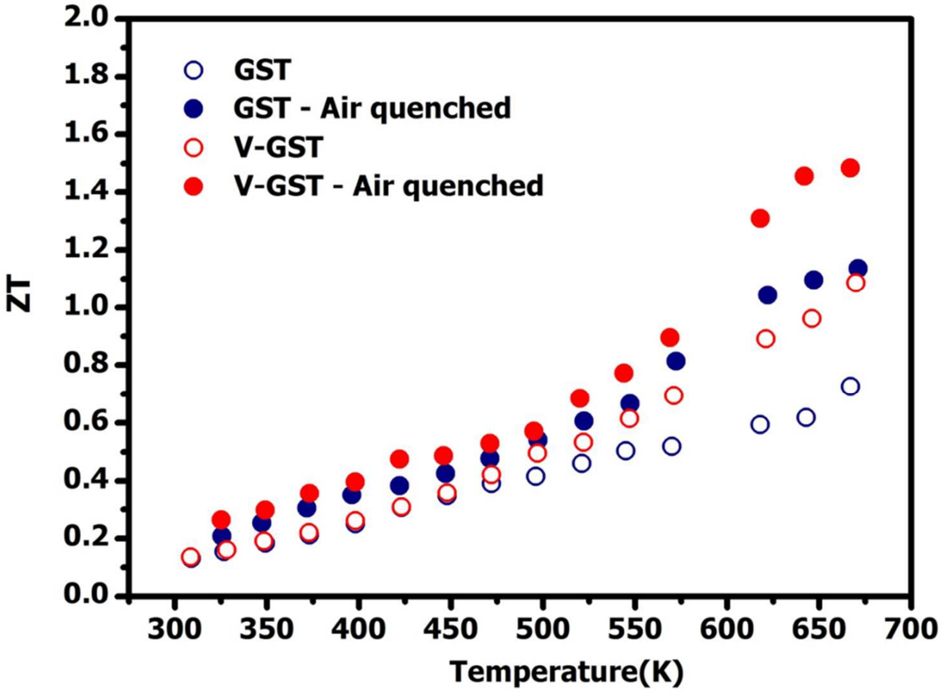

Fig. 4 Temperature dependence of thermoelectric figure of merit, ZT of GeTe-rich GeSbTe samples.

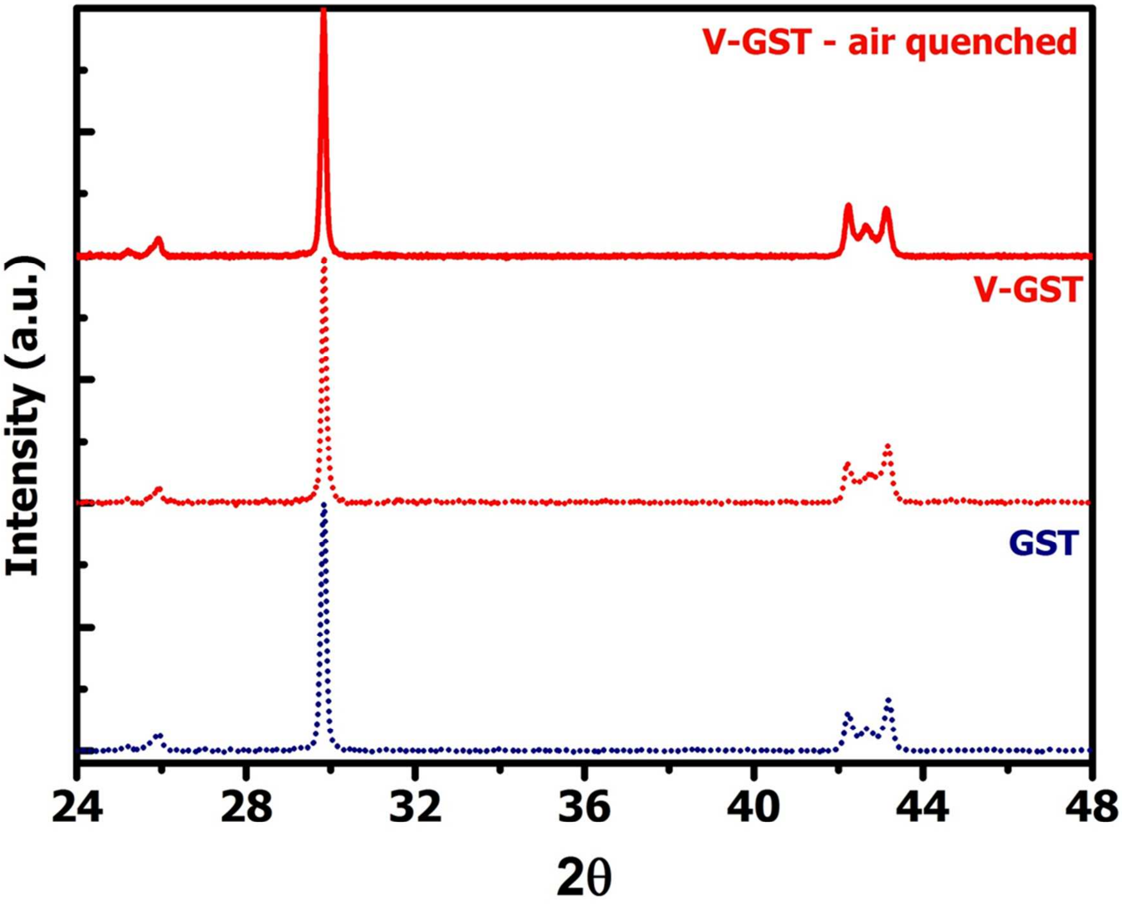

Fig. 5 Comparison of XRD patterns of the different GeTe-rich GeSbTe samples.

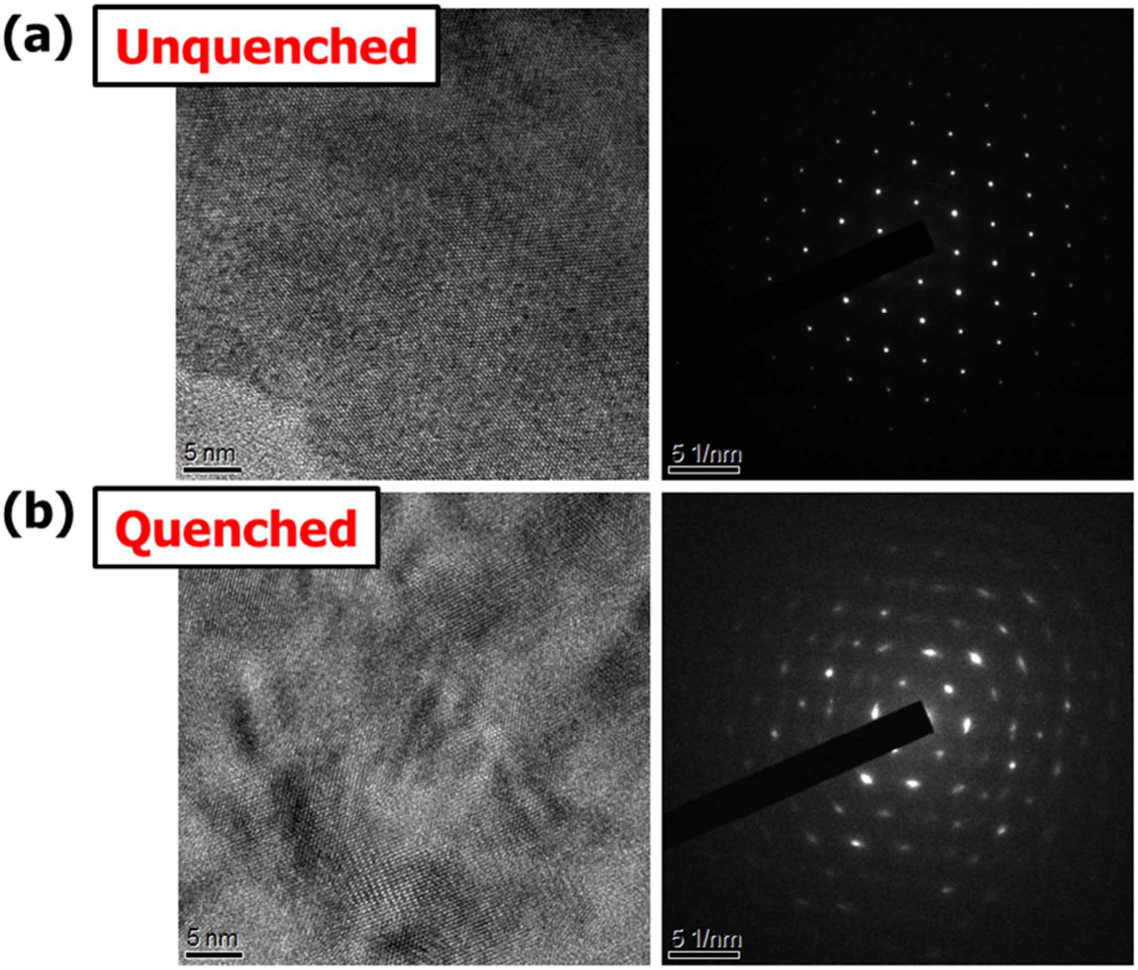

Fig. 6 HR-TEM image and corresponding SAED pattern of (a) unquenched V-GST and (b) quenched V-GST.

Table 1 Physical properties of the unquenched GeTe-rich GeSbTe alloys at room temperature (electrical conductivity, σ; carrier concentration, η; Hall mobility, μ; Seebeck coefficient, S; effective mass, m*/m0).

Sample Name	GST	V-GST
Nominal composition	$Ge_{0.87}Sb_{0.09}Te$	$Ge_{0.86}Sb_{0.09}Te$
EDS composition	$Ge_{0.92}Sb_{0.11}Te$	$Ge_{0.91}Sb_{0.09}Te$
σ (S/cm)	1180 (±15)	1117 (±2)
η (x 10^{20}) (cm^{-3})	2.25 (±1.11)	5.66(±3.68)
μ (cm^2/V-s)	38 (±13)	16 (±7)
S (μV/K)	86	93
m^*/m_0	1.59	3.18